To be presented at: Computers in Reciprocating Engines and Gas Turbines, IMechE HQ, London, 9−10 January 1996

M. Wilson, J. X. Chen and J. M. Owen
School of Mechanical Engineering
University of Bath, UK

Computation of flow and heat transfer in rotating−disc systems

SYNOPSIS

The flow in the internal cooling−air systems of gas turbines can be modelled using simple rotating−disc systems. In this paper, finite−volume methods and low Reynolds−number k−ε turbulence models are used to compute the flow and heat transfer between two confined discs with a radial outflow of cooling air. The two discs can rotate at different speeds and the systems can be characterised by the rotation ratio, Γ, of the slower to the faster disc. Computational results for axisymmetric, incompressible, steady flow are compared with data from purpose−built experimental rigs. The co−rotating (Γ=+1), rotor−stator (Γ=0) and contra−rotating (Γ=−1) disc systems discussed represent problems encountered in internal−air systems, and detailed understanding of the behaviour of these systems should lead to improvements in gas−turbine design with consequent improvements in efficiency.

NOTATION

a, b	inner and outer radius of disc respectively
C_m	moment coefficient (=M/0.5ρΩ²b⁵)
C_w	nondimensional flow rate (=m/μb)
C_p	specific heat capacity
G	gap ratio (=s/b)
k	turbulent kinetic energy, thermal conductivity
m	superposed mass flow−rate
M	moment on one side of disc
Nu	Nusselt number ($qr/k(T_{disc}-T_{ref})$)
Pr	Prandtl number
q	heat flux from disc to fluid
Re_ϕ, Re_t	rotational Reynolds number (=ρΩb²/μ), turbulence Reynolds number (=ρk^2/με)
r	radius
s, s_c	axial gap between discs, shroud clearance
S_r	swirl ratio of pre−swirl air (=$v_{\phi,p}/\Omega r_p$)
T	static temperature
U_τ	friction velocity
v_r, v_ϕ, v_z	mean−flow velocity components in r, ϕ, z directions
x	nondimensional radius (=r/b)
y,y^+	wall distance, nondimensional wall distance (=ρ$U_\tau y$/μ)
z	axial co−ordinate
β	core rotation ratio (=ω/Ω)
ε	turbulence energy dissipation rate
Γ	ratio of angular velocity of slower to faster disc
λ_T, λ_L	turbulent flow parameter (=$C_w Re_\phi^{-0.8}$), laminar flow parameter (=$C_w Re_\phi^{-0.5}$)

μ	dynamic viscosity
ρ	density
τ_w	total wall shear stress
ϕ	tangential co−ordinate
ω	angular speed of inviscid core
Ω	angular speed of disc

Subscripts

d,s,p,b	disc, seal, pre−swirl, blade−cooling air
ref	reference value
t	turbulent

1. INTRODUCTION

In gas−turbine engines, a small percentage of the air is bled from the compressor to cool the nozzle−guide vanes, turbine blades and turbine discs. Cooling poses a design dilemma: too much cooling air is expensive and inefficient but too little can result in the failure of expensive components.

The flow and heat transfer associated with rotating turbine discs can be complex and difficult to compute, and reliable experimental data are needed to validate the computer codes being developed for this purpose. Rotating−disc systems, in which a plane disc rotates next to another rotating or stationary disc, provide simple models of the more complex geometries that occur in engines: these models can then be used to produce experimental data to validate codes.

It is convenient to classify rotating−disc systems using the parameter Γ, which is the ratio of the angular speed of the slower disc to that of the faster disc: for all cases $-1 \le \Gamma \le +1$. Fig 1 shows simplified models of three important cases: the rotating cavity, Γ=+1; the rotor−stator system, Γ=0; contra−rotating discs, Γ=−1. The flow structure associated with the rotor−stator system (which represents a turbine disc rotating close to a stationary casing) and the rotating cavity (which represents two co−rotating turbine or compressor discs) are discussed extensively by Owen and Rogers (1,2).

This paper presents an overview, using both new and published results, of some recent applications of elliptic solvers, incorporating low Reynolds number k−ε turbulence models, to the computation of flow and heat transfer in rotating−disc systems for Γ=+1, 0 and −1. The experimental rigs and computational models are described in sections 2 and 3, and comparisons between computations and data are made in section 4. Conclusions and possible directions for future developments are given in section 5.

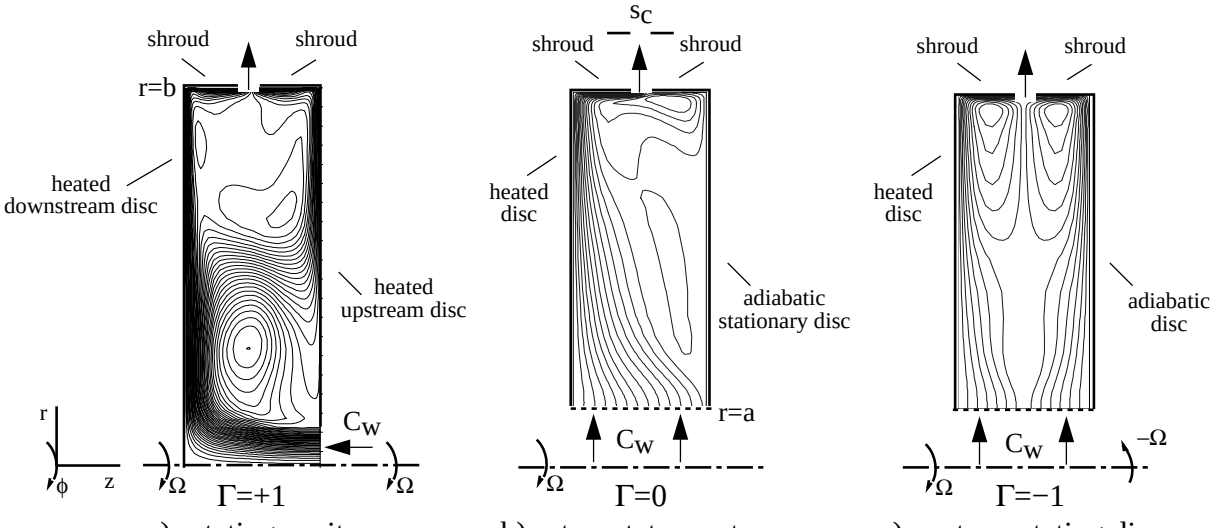

Fig. 1 Computational models and computed streamlines in rotating disc systems

2. EXPERIMENTAL RIGS AND SIMPLIFIED COMPUTATIONAL MODELS

2.1 Contra−rotating disc rig

The same experimental rig was used to make measurements of flow and heat transfer in both contra−rotating disc systems and for the rotor−stator configuration, the latter being the special case Γ=0. The apparatus was described by Gan et al (3) and Chen et al (4), and a brief summary is given here relevant to the computational models illustrated in Fig. 1b and Fig. 1c.

The rig comprised two discs, one of steel and one of transparent polycarbonate, which could be rotated independently up to 1500 rev/min. A peripheral shroud was attached to each disc using insulating material, giving an effective radius b=391 mm for the discs. The axial clearance s_c between the shrouds increased with speed and was estimated as 4 mm maximum, and the gap ratio for the cavity was G=0.12. A radial outflow of cooling air was supplied through gauze tubes of 100 mm diameter attached to the centre of the discs (a/b=0.128). For contra−rotating disc cases (Fig. 1c), a uniform radial flux was prescribed at $r=a$, based on the measured mass flow−rate and inlet air temperature. This was given inlet swirl to match the disc speeds, so that $v_\phi=\Omega a$ for $0 < z/s < 1/2$ and $v_\phi=-\Omega a$ for $1/2 < z/s < 1$. For the rotor−stator tests, the uniform radial flux at inlet was given zero swirl. Zero gradient conditions were applied at the axial clearance, except for the radial velocity which was prescribed from the superposed flow−rate and the area of the exit boundary. Low turbulence levels were associated with the inlet flow and did not affect the computed results, in view of the higher turbulence levels generated within the flow. No−slip conditions were imposed at solid surfaces.

Six thermocouples on the heated steel disc, located between x=0.2 and x=1.0, were used to provide fixed temperature boundary conditions, and six fluxmeters provided heat flux data for comparison with computational results. All other surfaces were assumed adiabatic. The transparent disc allowed LDA measurements to be made of radial and tangential velocity distributions between the discs. More details are given by Gan et al (3).

2.2 Pre−swirl rotor−stator rig

Wilson et al (5) gave a detailed description of an experimental rig used to study a direct transfer pre−swirl system. This comprised a rotor−stator system with a radial outflow of cooling air, separated by an inner seal from an axial cross−flow of cold air. A schematic diagram of the rig and the two superposed flows is given in Fig. 2.

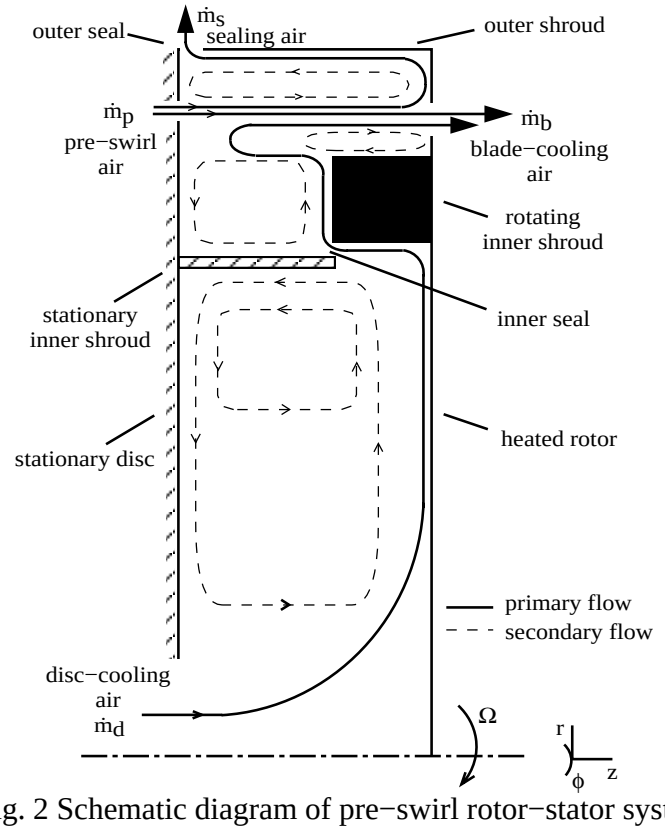

Fig. 2 Schematic diagram of pre−swirl rotor−stator system

The maximum rotational Reynolds number tested was $Re_\phi \approx 2.0 \times 10^6$ at 7000 rev/min, based on the outer seal centreline radius b=215 mm (G=0.103). The cross−flow entered the pre−swirl chamber, formed by the inner and outer seals, from sixty pre−swirl nozzles on the stationary disc (at a radius r_p=200 mm and angled at 20° to the tangential direction) and left through sixty blade−cooling holes on the rotor. In the computational model, the discrete pre−swirl nozzles and blade−cooling holes were represented by equivalent−area annular slots, giving a steady axisymmetric approximation to the real (3D time−dependent) system. Inlet velocities were deduced from measured mass flow−rates, and inlet temperatures were also known. The flow−rates in the experiment could be balanced so that $C_{w,b}=C_{w,p}$ and $C_{w,s}=C_{w,d}$, and this was used to divide the mass−flow leaving the system between the blade−cooling slot and the outer seal. The latter was repesented by an axial clearance between the rotor and the stationary outer shroud. Full details of modelling simplifications were given by Wilson et al (5).

The temperature of the heated disc was measured by six thermocouples located at $0.3 < x < 1$, and a polynomial fit to these data provided fixed temperature boundary conditions for the disc. Similar use was made of temperatures measured on the stator for $0.23 < x < 0.85$. Heat flux through the disc was measured by fluxmeters with radial locations at $0.65 < x < 1$. One of these was located under the inner shroud on the rotating disc (at x=0.86), and this measurement was used to distribute a constant heat flux around the surface of the shroud. It was not possible to make use of the measurement underneath the outer shroud in the simplified model.

Adiabatic surfaces were assumed wherever information was not available, including the stationary shrouds and the stator surface in the pre−swirl chamber. Computed results could be compared with tangential velocities and temperatures measured at eight radial locations on the mid−plane between the discs (z/s=0.5): this included one point inside the pre−swirl chamber at $x \approx 0.84$. The temperature of the air entering the blade−cooling holes was also measured.

The validation of models for flow and heat transfer in rotor−stator systems is clearly of importance in relation to the pre−swirl system described above. In an alternative configuration (now being studied experimentally), pre−swirl air flows radially outward between the heated disc and a rotating cover−plate mounted at the mid−plane (z/s=1/2). For this case, verification of codes against data for heated rotating cavities is of interest, and this is also described below.

3. COMPUTATIONAL METHOD

3.1 Finite−volume method

Numerical solutions have been obtained, using iterative pressure−correction methods, to discretised forms of the axisymmetric, steady, incompressible Reynolds−averaged Navier−Stokes and energy equations, in primitive variables, using hybrid−upwind differencing on a cylindrical−polar grid, and with staggered storage locations for the axial and radial components of velocity. In the k−ε turbulence closure used here, turbulent diffusion is represented by a turbulent viscosity μ_t, computed from local values of k and ε, and with turbulent heat flux computed using a turbulent Prandtl number. Two different (but closely related) turbulence model formulations have been tested.

The rotating cavity and pre−swirl computations described below were carried out using a multigrid solver described by Gan et al (6) with the Launder and Sharma (7) low Reynolds number k−ε turbulence model. The multigrid code was developed from that described by Vaughan, Gilham and Chew (8). Rotor−stator and contra−rotating disc computations were carried out using a single−grid solver with a low Reynolds−number k−ε turbulence model developed by Morse (9). This code was described by Chen et al (4).

3.2 Turbulence models

Launder and Sharma (7) devised a low Reynolds number k−ε turbulence model, for application to flow near a spinning disc, which includes terms in the turbulence transport equations representing the effect of molecular viscosity on turbulence structure near walls. The model also predicts transition from laminar to turbulent flow, and turbulence levels near the wall are reduced by damping of the turbulent viscosity μ_t, using an exponential function based on local turbulence Reynolds number, Re_t. Morse (9) found that the Launder and

Sharma model exhibited delayed transition to turbulence in free−disc and rotating cavity flows, and modified the model using a damping function based on dimensionless distance from the wall, y^+. The two models generally return similar results for cases where transitional effects are small.

Low Reynolds number models can give accurate predictions of flow and heat transfer over a range of rotating−disc problems, as described below, however approximately double the number of grid−points are required than would be needed to apply a high Reynolds number model with wall−functions. This is because the model needs to be applied in the laminar sub−layer very close to the wall, where the non−dimensional distance y^+ is less than unity.

4. COMPARISON BETWEEN COMPUTATIONS AND EXPERIMENTAL DATA

4.1 Rotating cavity with radial outflow (Γ=+1)

Computations were carried out (by I. Mirzaee, University of Bath) using the multigrid solver for comparison with tangential velocities, measured by Pincombe (10), on the radial mid−plane of a rotating cavity with $5.4\text{x}10^5 < Re_\phi < 1.1\text{x}10^6$ and $C_w \approx 2500$. A uniform axial flux at inlet was assumed (as illustrated in Fig. 1a) with $v_\phi/\Omega r=1$, and a 91 by 115 axial by radial grid was used. Fig. 3a shows the measured tangential velocities plotted against x^{-2}, illustrating that the data for each case follow a Rankine vortex behaviour:

$$v_\phi/\Omega r = A + Bx^{-2} \;;\; A, B \text{ constant} \qquad (1)$$

The computed results show that this behaviour is reasonably well captured by both the Launder and Sharma and Morse turbulence models (for laminar flow, the computed results agreed with the exact solution of the Ekman layer equations, for which $A=1$ and $B=\lambda_l/2\pi$).

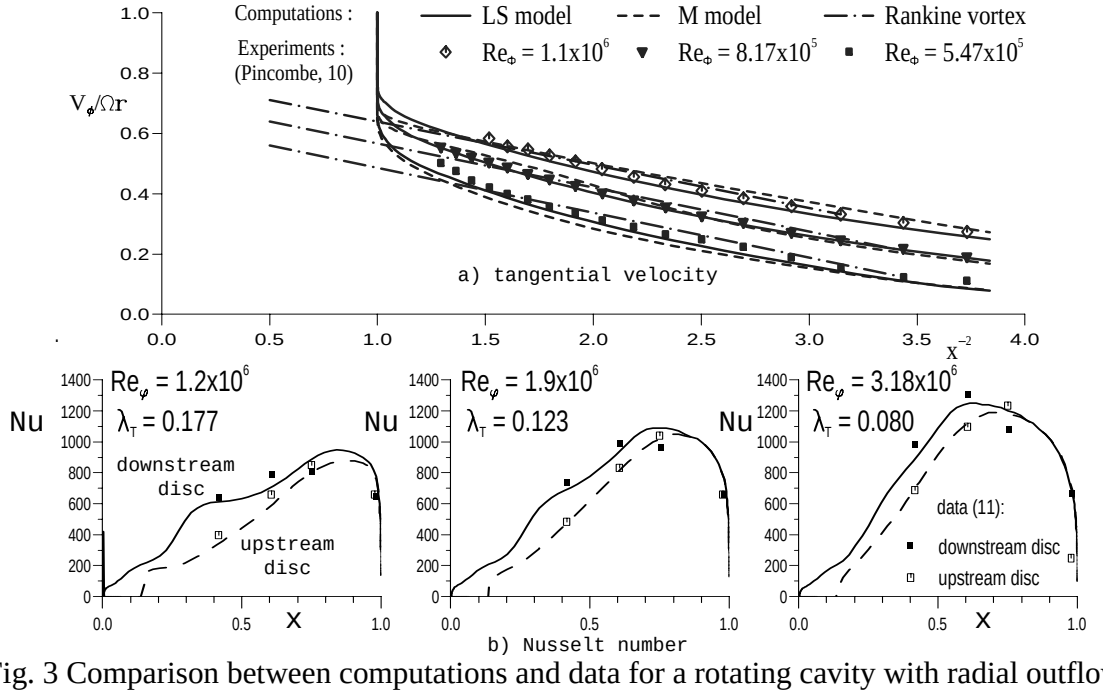

Fig. 3 Comparison between computations and data for a rotating cavity with radial outflow

Heat transfer computations were carried out (by H. Karabay, University of Bath), using the Launder and Sharma turbulence model, for comparison with the Nusselt number distributions reported by Northrop and Owen (11) for a rotating cavity with symmetrically heated discs, using the original data to prescribe inlet flow boundary conditions and to supply the temperature distributions for the two discs. Computational results for Nusselt number Nu are shown in Fig. 3b, in comparison with data for cases with $1.2\text{x}10^6 \le Re_\phi \le 3.18\text{x}10^6$ and $C_w \approx 13000$. The reference temperature used for the Nusselt numbers is the adiabatic disc temperature:

$$T_{ref} = T_d + 1/2 Pr^{1/3} \Omega^2 r^2 / Cp \qquad (2)$$

For cases with $\lambda_T < 0.2$, the peak Nusselt number on the downstream disc shows the end of the predicted source region, where all the flow has been entrained by the boundary layers: the non−entraining Ekman−type layer radially outward of the source region gives rise to reduced heat transfer.

The agreement between computations and data shown in Fig. 3b is reasonably good in most cases, although for $Re_\phi > 10^6$ the Nusselt numbers on the downstream disc are overpredicted in the outer part of the cavity, and the upstream disc values are slightly underpredicted. The agreement is similar to that obtained by Morse and Ong (12) who computed these cases using the Morse turbulence model.

4.2 Rotor−stator system with radial outflow (Γ=0)

A modified version of the Morse (9) turbulence model was used by Chen et al (4) to compute heat transfer cases for comparison with data from the rotating−disc rig described in section 2.1. A 92 by 76 axial by radial grid was used, contracted to the walls and with $y^+ < 0.5$ for application of the turbulence model. Grid refinement was also used around the mid−plane between the discs, in order to resolve the flow leaving at the shroud clearance (Fig. 1b). There was no significant difference between solutions obtained with this grid and one with double the number of points in each direction.

Fluid dynamics computations were verified by comparing predicted velocity distributions with measurements obtained at $Re_\phi = 1.25 \times 10^6$, $C_w = 6100$ ($\lambda_T = 0.08$) for $G = 0.12$. The results are reproduced in Fig. 4 for radial locations with $0.6 < x < 0.85$ at which data were available. The peak radial velocity near the disc is slightly overpredicted, and the tangential velocity of the rotating core is underpredicted, but the general level of agreement is reasonable. The computed results at the lowest radius (x=0.6) are sensitive to the assumed inlet boundary conditions (section 2.1). The tangential velocity of the rotating core of fluid between the discs is reduced, relative to an enclosed rotor−stator system, due to the superposed flow with zero inlet swirl, and this increases the disc frictional moment.

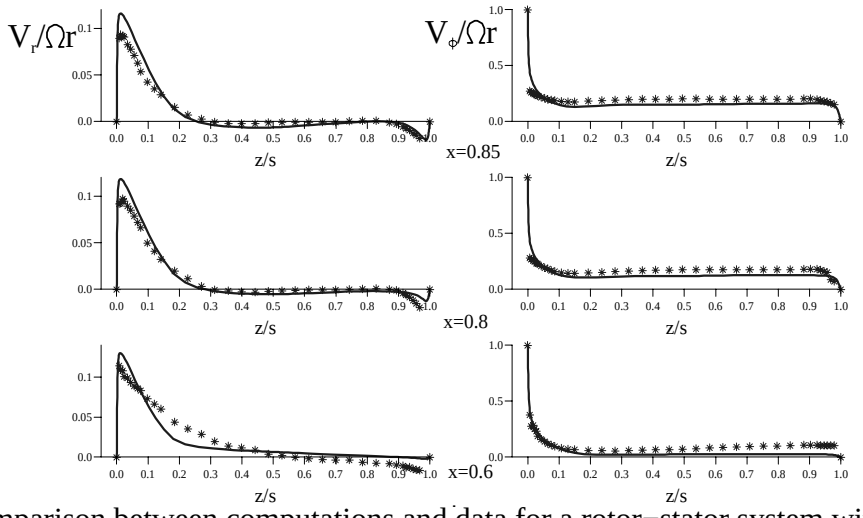

Fig. 4 Comparison between computations and data for a rotor−stator system with radial outflow $Re_\phi = 1.25 \times 10^6$, $C_w = 6100$ ($\lambda_T = 0.08$), $G = 0.12$

For "wide gap" cases (with separate boundary layers on the discs), Daily et al (13) correlated the moment coefficients as:

$$C_m = C_m^*(1 + 13.9\beta^*\lambda_T G^{-1/8}) \;;\; C_m^* = 0.0510 G^{0.1} Re_\phi^{-0.2} \;;\; \beta^* = 0.43 \qquad (3)$$

where C_m^* and β^* are the moment coefficient and core rotation ratio for the corresponding enclosed system ($\lambda_T = 0$). The correlation gives a value $C_m = 4.08 \times 10^{-3}$ for the case described above, and the computations gave $C_m = 3.80 \times 10^{-3}$ (the Launder and Sharma model gave an almost identical result). The value of C_m^* is about half that for a free−disc, and C_m rises toward the free−disc value as $\lambda_T \rightarrow 0.22$, the free−disc entrainment rate. The effect of C_w on computed velocity distributions was studied parametrically by Chen et al (4).

Four heat transfer cases were computed at Re_ϕ=1.25x10^6, with C_w=2530, 3900, 6100 and 9680 ($0.03 < \lambda_T < 0.13$), using the same grid as above. The computed Nusselt numbers for the four cases followed the measured trend of increasing heat transfer with increasing C_w, and agreed reasonably well with the experimental data corrected for the effects of radiation, as described by Chen et al (4). The agreement improved as C_w increased, and it is thought that the radiation correction is more accurate at high C_w, where the ambient temperature should be better approximated by the superposed flow inlet temperature. The Nusselt numbers for the highest flow−rate case ($\lambda_T \approx 0.13$) were similar to those measured during free−disc tests (λ_T=0.22) away from the effects of the source region. Other results for heat transfer in a rotor−stator system are presented below.

4.3 Contra−rotating discs with radial outflow (Γ=−1)

Comparisons between computed and measured velocity profiles for Γ=−1, Re_ϕ=1.14x10^6, C_w=4026 ($\lambda_T \approx 0.057$) are shown in Fig. 5a. These computations were carried out by Chen et al (14) using a 92 by 78 grid (with $y^+<1$ for the grid−node closest to the discs) and a modified Morse (9) turbulence model: many other comparisons were presented by Gan et al (3) and Gan et al (6) using the Launder and Sharma model, for which very similar results were obtained. The computations and data in Fig. 5a agree well, with the exception of the radial velocity near z/s=1 where measurements were difficult to make. The radial velocity distributions show recirculating flow in the mid−plane at x=0.6, indicating that these comparisons are made outside the source region (Fig. 1c). Gan et al (6) reported computations at higher values of λ_T which showed that the Launder and Sharma turbulence model tended to overpredict the radial extent of the source region (these comparisons with data were carried out at lower rotational Reynolds numbers, $Re_\phi \approx 3.8\text{x}10^5$, where turbulent transition is more influential). Disc moment coefficients were not measured, but computed results showed that C_m was close to the free−disc value and insensitive to changes in superposed flow−rate. The results were also within about 2% of earlier predictions by Morse (15) for cases with $1.25\text{x}10^6 \le Re_\phi \le 10^7$.

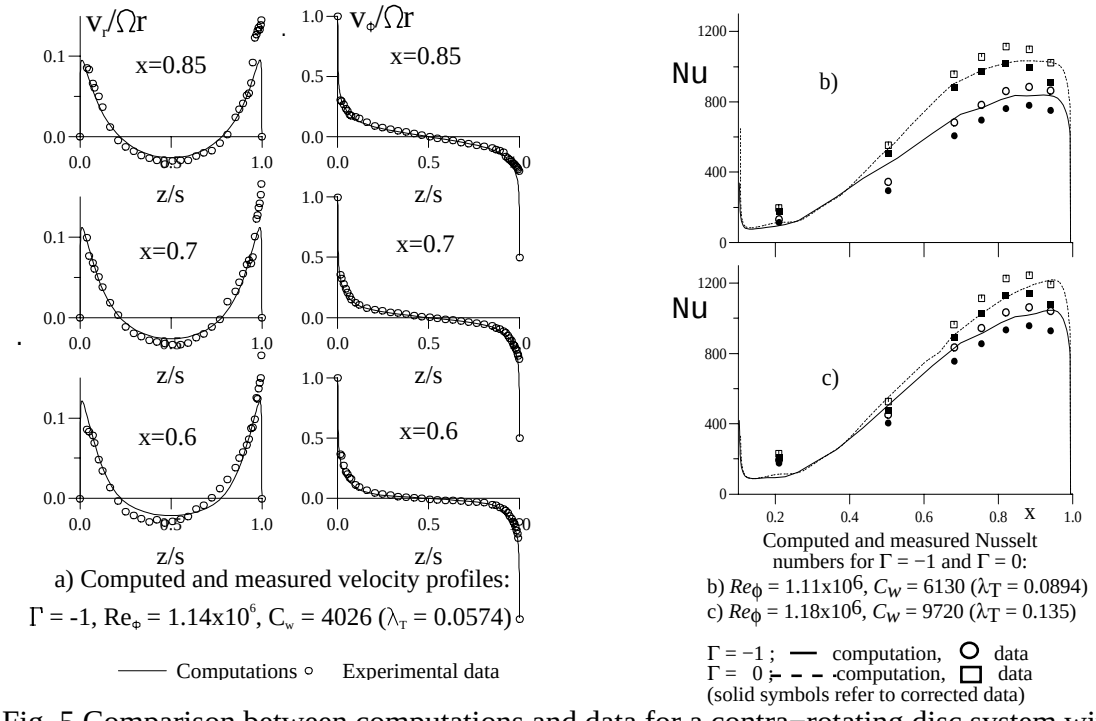

a) Computed and measured velocity profiles:
Γ = -1, Re_ϕ = 1.14x10^6, C_w = 4026 (λ_T = 0.0574)

Computed and measured Nusselt numbers for Γ = −1 and Γ = 0:
b) Re_ϕ = 1.11x10^6, C_w = 6130 (λ_T = 0.0894)
c) Re_ϕ = 1.18x10^6, C_w = 9720 (λ_T = 0.135)

Γ = −1 ; — computation, ○ data
Γ = 0 ; - - - computation, □ data
(solid symbols refer to corrected data)

Fig. 5 Comparison between computations and data for a contra−rotating disc system with a radial outflow

Chen et al (14) compared computed and measured Nusselt numbers for a number of cases with $2\text{x}10^5 < Re_\phi < 1.11\text{x}10^6$ and $0.089 < \lambda_T < 0.51$. The adiabatic disc was predicted to remain at the inlet air temperature until the end of the source region, x_e. Gan et al (3) applied the known free−disc entrainment rate to both discs to estimate this as:

$$x_e = 1.37\lambda_T^{0.385} \qquad (4)$$

This agreed well with the predicted location in the cases considered by Chen et al (14). The temperature of the recirculating air in the mid−plane was found to be higher than that of the unheated disc.

Fig. 5b,c shows comparisons between computed and measured Nusselt numbers for both $\Gamma=-1$ and $\Gamma=0$ (the rotor−stator system) at equivalent test conditions. Reasonable agreement is obtained for $x>0.6$ (beyond the effects of the source region) with experimental data corrected for radiation effects. The heat transfer in the contra−rotating disc system is lower than that for the corresponding rotor−stator case, due to the recirculation of hot fluid in the non−rotating core flow between the discs. There is no recirculation in the rotating core for $\Gamma=0$.

4.4 Pre−swirl rotor−stator system ($\Gamma=0$)

The computed streamlines shown in Fig. 6a,b illustrate the flow patterns inside the pre−swirl chamber of the system described in section 2.2 and shown schematically in Fig. 2. The computations were carried out by Wilson et al (5) at $Re_\phi=1.23\text{x}10^6$ and $C_{w,d}\approx2250$ ($\lambda_T\approx0.06$) using the Launder and Sharma turbulence model on a 115 by 323 grid: block obstructions within the grid represented the inner shrouds. Comparison between Fig. 6a and Fig. 6b shows the predicted effect of doubling the pre−swirl flow−rate, from $C_{w,p}/C_{w,d}=2.18$ to 4.52 (the swirl ratio also changes as a consequence, from S_r about 1 to S_r about 2). In Fig. 6a, the pre−swirl cross−flow causes toroidal recirculations above and below the cross−flow centreline. The disc cooling air flows radially outward from the inner system and into the pre−swirl chamber through the inner seal. The boundary layer remains attached to the disc as it flows around the rotating shroud, and is ingested into the blade−cooling slot at x≈0.93. No reverse flow (from the pre−swirl chamber to the inner system) occurs at the inner seal in the predictions.

When the pre−swirl flow−rate is doubled (Fig. 6b), the disc−cooling air boundary layer separates from the top of the rotating inner shroud, and is ingested into the blade−cooling slot by entrainment into the under−side of the cross−flow. Chen et al (16,17) carried out three−dimensional laminar flow computations of a simplified pre−swirl system which showed that these "direct" or "indirect" routes for ingestion of disc−cooling air (Fig. 6a and Fig. 6b respectively) affected the temperature of the air at the blade−cooling holes.

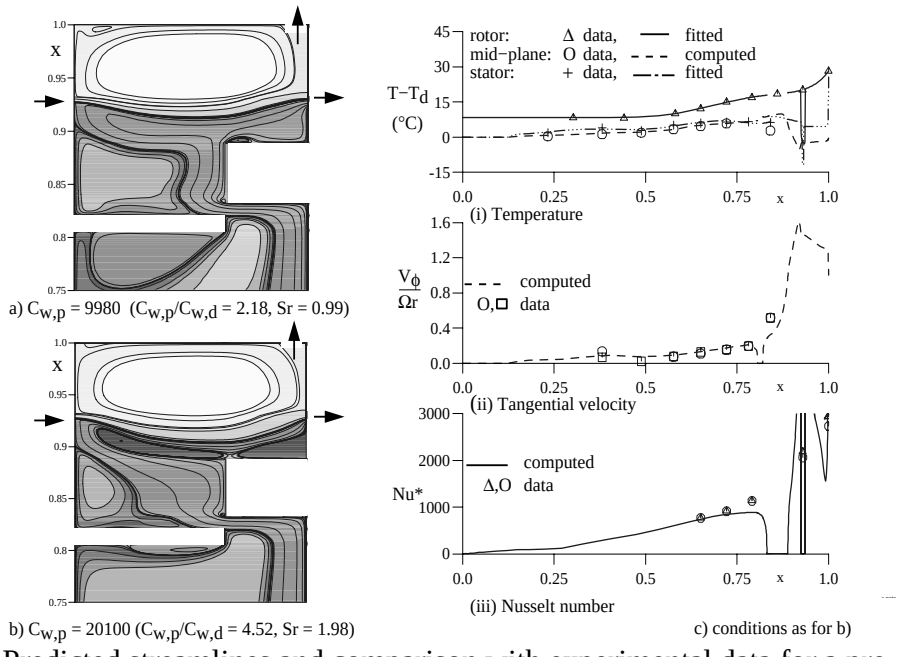

Fig. 6 Predicted streamlines and comparison with experimental data for a pre−swirl rotor−stator system, $Re_\phi=1.23\text{x}10^6$, $C_{w,d}\approx2250$ ($\lambda_T\approx0.06$)

The two computations described above were carried out by Wilson et al (5) in order to make comparisons with measurements from two of the tests in an extensive experimental programme. Fig. 6c shows these comparisons for the case illustrated in Fig. 6b. Fig. 6c(i)

shows the fitted temperatures used as boundary conditions on the rotor and stator, and the computed mid−plane air temperature. The mid−plane temperature is well predicted in the inner rotor−stator system, but there is insufficient data to validate properly the computation of the interacting flows in the pre−swirl chamber. The same comments apply to the computed mid−plane tangential velocities shown in Fig. 6c(ii). Fig. 6c(iii) shows that the measured Nusselt numbers in the inner system are slightly underpredicted. The high values for Nu for x>0.82 approximately (i.e. inside the pre−swirl chamber) are due to the impingement of the cross−flow on the disc: no direct comparison could be made between the computed results from the axisymmetric model and the measurement made between the blade−cooling holes on the disc at x=0.93.

The measured (and computed) Nusselt numbers in the inner system were found to be virtually identical for the two cases illustrated in Fig. 5a and Fig. 5b, suggesting that no reverse flow occurred at the inner seal. Similar computations, carried out at a lower disc−cooling air flow−rate ($\lambda_T \approx 0.03$), did show an effect of increased pre−swirl flow−rate on the Nusselt numbers in the inner system, but the computed results again showed no effect. These results were discussed in more detail by Wilson et al (5).

Computed values of air temperature rise, from pre−swirl inlet to blade−cooling exit, were found to be consistently underpredicted by about 30% (corresponding to around 2°C) compared with measured values, although the trends of the experimental data were correctly reproduced for the cases considered. The individual effects of geometrical and axisymmetric simplifications in the model, turbulence model deficiencies in predicting the recirculating, impinging flow in the pre−chamber, and sensitivity to assumed thermal boundary conditions have yet to be explored, and many more experimental data−sets are available for the further studies required to bring about improvements in prediction of the air temperature rise.

5. CONCLUSIONS

Low Reynolds number k−ε turbulence models have been shown to give sufficiently good agreement with experimental data for flow and heat transfer in different classes of rotating−disc systems with a radial outflow of cooling air, for rotational Reynolds numbers up to 3.8×10^6, although around 1.25×10^6 for most of the cases discussed. Other workers have found that more economical turbulence models, using mixing−length models or wall−functions near solid surfaces, do not give the same level of agreement with heat transfer data for the range of systems with Γ=+1, 0 and −1. The need to carry out computations at higher rotational Reynolds numbers for practical applications to gas−turbines (where $Re_\phi \approx 10^7$), to model flows with strong axial flow and recirculation such as the pre−swirl problem, and to compute systems involving radial inflow rather than outflow, all pose additional difficulties which will require further validation, and testing of alternative turbulence models. The work described in this paper should provide useful results to assess more sophisticated models, as well as the less computationally−demanding models which may be required for designs involving fully three−dimensional rotating−disc flows.

5. ACKNOWLEDGEMENTS

The experimental and computational work described above has been sponsored by EPSRC, European Gas Turbines Ltd,. Motoren und Turbinen Union and DRA. The rotating cavity computations were carried out at the University of Bath by Mr H. Karabay and Mr I. Mirzaee who are funded by the Turkish and Iranian governments respectively.

REFERENCES

(1) OWEN, J.M. and ROGERS, R.H. Flow and heat transfer in rotating disc systems: vol. 1, rotor−stator systems, 1989 (Research Studies Press, Taunton, U.K. and John Wiley, New York, USA)

(2) OWEN, J.M. and ROGERS, R.H. Flow and heat transfer in rotating disc systems: vol. 2,

rotating cavities, 1995 (Research Studies Press, Taunton, U.K. and John Wiley, New York, USA)

(3) GAN, X., KILIC, M. and OWEN, J. M. Flow between contra−rotating discs, ASME Paper 93−GT−286, 1993 (To be published in J.Turbomachinery)

(4) CHEN, J−X., GAN, X. and OWEN, J.M. Heat transfer in an air−cooled rotor−stator system, ASME Paper 94−GT−55, 1994 (To be published in J. Turbomachinery)

(5) WILSON, M., PILBROW, R. and OWEN, J.M. Flow and heat transfer in a pre−swirl rotor−stator system, ASME Paper 95−GT−239, 1995 (To be published in J. Turbomachinery)

(6) GAN, X., KILIC, M. AND OWEN, J. M. Superposed flow between two discs contrarotating at differential speeds, Int. J. Heat and Fluid Flow, 1994, 15, 438−446

(7) LAUNDER, B. E. and SHARMA, B. I. Application of the energy−dissipation model of turbulence to flow near a spinning disc, Letters in Heat and Mass Transfer, 1974, 1, 131−138

(8) VAUGHAN, C. M., GILHAM, S. and CHEW, J.W. Numerical solutions of rotating disc flows using a non−linear multigrid algorithm, Proc. 6th Conf. Num. Meth. Lam. Turb. Flow, 1989, (Pineridge Press, Swansea), 66−73

(9) MORSE, A.P. Application of a low Reynolds number k−ε turbulence model to high−speed rotating cavity flows, J. Turbomachinery, 1991, 113, 98−105

(10) PINCOMBE, J. R. Optical Measurements of the flow inside a rotating cylinder, D.Phil thesis, 1983, University of Sussex

(11) NORTHROP, A and OWEN, J. M. Heat transfer measurements in rotating disc systems part 2: the rotating cavity with a radial outflow of cooling air. Int. J. Heat Fluid Flow, 1988, 9, 27−36

(12) MORSE, A.P. and ONG, C.L. Computation of heat transfer in rotating cavities using a two−equation model of turbulence, J. Turbomachinery, 1992, 114, 247−255

(13) DAILY, J. W., ERNST, W. D. and ASBEDIAN, V. V. Enclosed rotating discs with superimposed throughflow, 1964, Dept. Civil Engng, Hydrodyn. Lab MIT Rep. No.64

(14) CHEN, J−X., GAN, X. and OWEN, J.M. Heat transfer from air−cooled contra−rotating discs ASME Paper 95−GT−184, 1995 (To be published in J. Turbomachinery)

(15) MORSE, A.P. Assessment of laminar−turbulent transition in closed disc geometries, J. Turbomachinery, 1991, 113, 131−138

(16) CHEN, J. X., OWEN, J. M. and WILSON, M. Parallel computing techniques applied to rotor−stator systems: fluid dynamics computations, Proc. 6th Conf. Num. Meth. Lam. Turb. Flow, 1993a, (Pineridge Press, Swansea), 899−911

(17) CHEN, J. X., OWEN, J. M. and WILSON, M. Parallel computing techniques applied to rotor−stator systems: thermal computations, Proc. 8th Int. Conf. Num. Meth. in Thermal Problems, 1993b, (Pineridge Press, Swansea), 1212−1226